BIOCHEMISTRY
including biophysical chemistry & molecular biology

Article

pubs.acs.org/biochemistry

Slow Unfolding Pathway of Hyperthermophilic Tk-RNase H2 Examined by Pulse Proteolysis Using the Stable Protease Tk-Subtilisin

Jun Okada,[†] Yuichi Koga,[†] Kazufumi Takano,*[,†,‡] and Shigenori Kanaya[†]

[†]Department of Material and Life Science, Osaka University, 2-1 Yamadaoka, Suita, Osaka 565-0871, Japan

[‡]Department of Biomolecular Chemistry, Kyoto Prefectural University, 1-5 Hangi-cho, Shimogamo, Sakyo-ku, Kyoto 606-8522, Japan

Supporting Information

ABSTRACT: The unfolding speed of some hyperthermophilic proteins is significantly slower than those of their mesostable homologues. Ribonuclease H2 from the hyperthermophilic archaeon *Thermococcus kodakarensis* (Tk-RNase H2) is stabilized by its remarkably slow unfolding rate. In this work, we examined the slow unfolding pathway of Tk-RNase H2 by pulse proteolysis using a superstable subtilisin-like serine protease from *T. kodakarensis* (Tk-subtilisin). Tk-subtilisin has enzymatic activity in highly concentrated guanidine hydrochloride (GdnHCl), in which Tk-RNase H2 unfolds slowly. The native state of Tk-RNase H2 was completely resistant to Tk-subtilisin, whereas the unfolded state (induced by 4 M GdnHCl) was degraded by Tk-subtilisin. Degradation products of Tk-RNase H2 created from pulse proteolysis during its unfolding were detected by tricine−sodium dodecyl sulfate−polyacrylamide gel electrophoresis. We identified the cleavage sites in Tk-RNase H2 by N-terminal sequencing and mass spectrometry and constructed mimics of the unfolding intermediate of Tk-RNase H2 by protein engineering. The mimics were biophysically characterized. We found that the native state of Tk-RNase H2 (N-state) changed to the I_A-state that was digested by Tk-subtilisin in the early stage of unfolding. In the slow unfolding pathway, the I_A-state shifted to two intermediate forms, I_B-state and I_C-state. The I_B-state was digested by Tk-subtilisin in the C-terminal region, but the I_C-state was a Tk-subtilisin resistant form. These states gradually unfolded through the I_D-state, in which the N-terminal region was digested. The results indicate that pulse proteolysis, by a superstable protease, was a suitable strategy and an effective tool for analyzing intermediate structures of proteins with slow unfolding properties. We also showed that the N-terminal region contributes to the slow unfolding of Tk-RNase H2, and the C-terminal region is important for folding and stability.

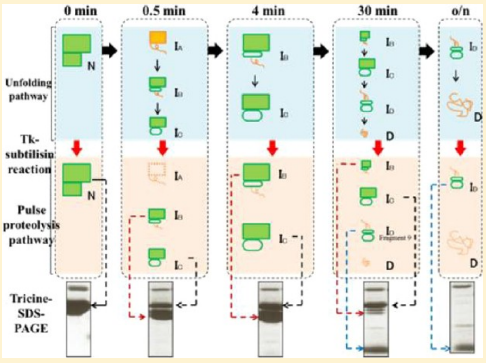

Proteins have a variety of intermediate structures during the transition between the unfolded and native states. Observing the intermediate structures contributes to our understanding of protein folding and unfolding.[1−4] Biophysical techniques such as circular dichroism (CD), fluorescence spectroscopy, small-angle X-ray scattering, and nuclear magnetic resonance (NMR) spectroscopy allow us to monitor intermediate structures during conformational changes induced by thermal or chemical denaturation.[5−11] Unfortunately, protein folding and unfolding are generally fast, and most intermediate structures are temporary and difficult to detect. Recent research in the field has indicated that some proteins from hyperthermophiles are stabilized by their remarkably slow unfolding rate.[12−23] Therefore, we are able to detect the intermediates of these proteins because of their slow unfolding.

Many hyperthermophilic proteins have considerable kinetic stability as measured by their high activation energy and slow unfolding kinetics.[12−23] Well-studied examples are pyrrolidone carboxyl peptidase from the hyperthermophilic archaeon *Pyrococcus furiosus* (Pf-PCP) and ribonuclease H2 from the hyperthermophilic archaeon *Thermococcus kodakarensis* (Tk-RNase H2). The unfolding rate of Pf-PCP is 10^7 times slower than that of mesophilic PCP from *Bacillus amyloliquefaciens*.[13] Iimura et al. observed high cooperativity among some intermediates of Pf-PCP by directly monitoring individual amino acid residues using real-time NMR.[24] Tk-RNase H2 is highly stable, with a stabilization mechanism characterized by a remarkably slow unfolding.[25] Using hydrophobic and proline mutant proteins of Tk-RNase H2, hydrophobic effects were shown to be a reason for the slow unfolding, but the proline residues had no effect.[26−28] Comparison of forms of RNase H from hyperthermophilic archaea with forms of RNase H2 from hyperthermophilic bacteria showed these proteins have different unfolding rates. Tk-RNase H2 and RNase H1 from *Sulfolobus tokodaii* unfold more slowly than RNase H2 from *Thermotoga maritima* (Tm-RNase H2) and RNase H2 from *Aquifex aeolicus*.[29]

Received: July 19, 2012
Revised: October 24, 2012
Published: October 29, 2012

   dx.doi.org/10.1021/bi300973n | *Biochemistry* 2012, 51, 9178−9191

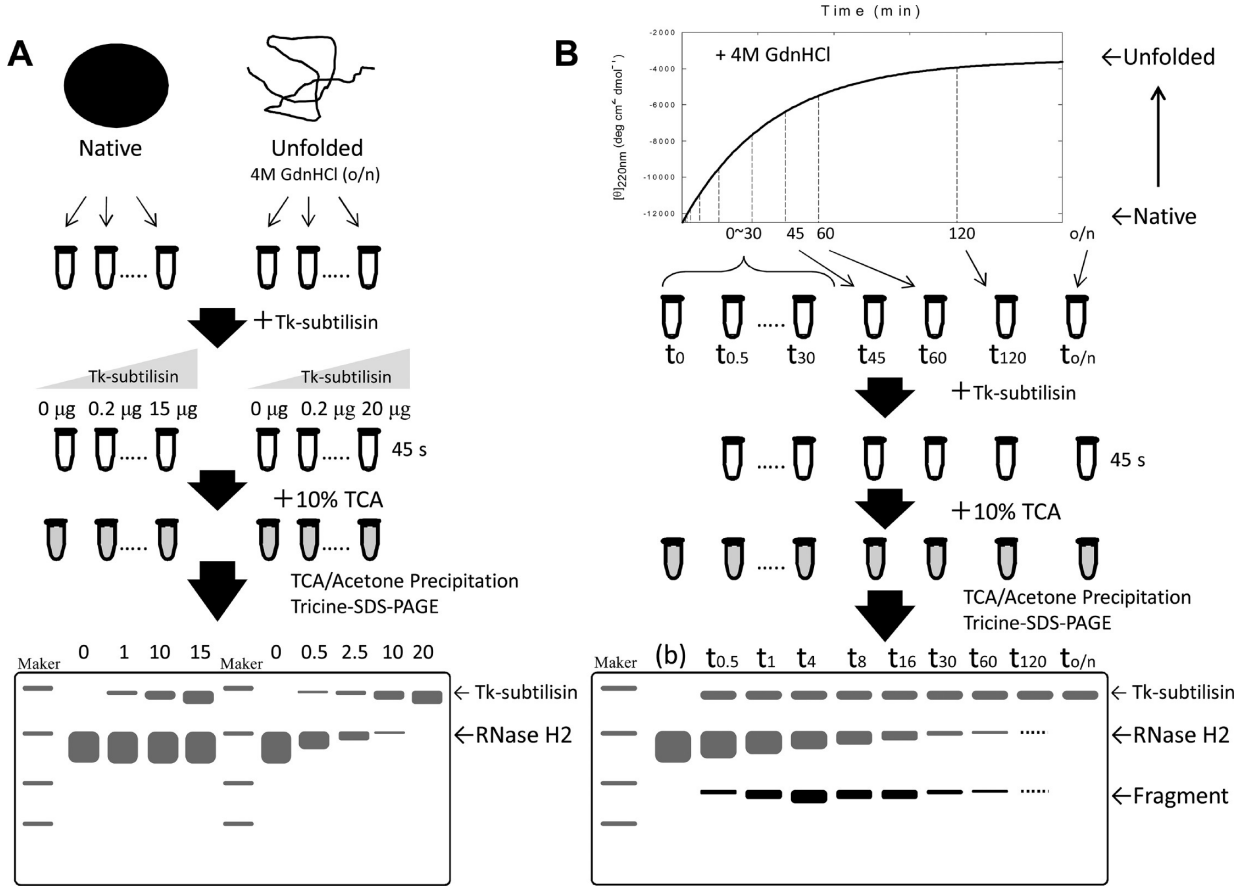

Figure 1. Schematic diagram of pulse proteolysis. (A) Pulse proteolysis of native and unfolded proteins by Tk-subtilisin. Native protein and unfolded protein were dispensed into tubes. Proteolysis was performed via addition of Tk-subtilisin (0–20 μg) and incubation for 45 s. The reaction was quenched by 10% TCA, and the products were quantified by tricine–SDS–PAGE. (B) Pulse proteolysis of kinetic unfolding by Tk-subtilisin. The native protein was unfolded by 4 M GdnHCl. At each time point, the sample was dispensed into a tube, and proteolysis was performed and analyzed as described for panel A.

In this study, we monitored the intermediate structures of Tk-RNase H2 in the slow unfolding pathway using pulse proteolysis and a superstable protease in the presence of the denaturant guanidine hydrochloride (GdnHCl). Subtilisin from the hyperthermophilic archaeon *T. kodakarensis* (Tk-subtilisin) is a protease with high stability and activity in high temperatures as well as in the presence of chemical denaturants.[30] Figure 1 shows the experimental procedures for pulse proteolysis used in this work. We successfully identified the regions that constitute the kinetic unfolding intermediates and observed the unfolding behavior of Tk-RNase H2. The results indicated that Tk-RNase H2 included multiple intermediate forms during the unfolding process. However, we did not find these intermediates in Tm-RNase H2. On the basis of the results obtained, we discuss the origin of slow unfolding of Tk-RNase H2. We also show that pulse proteolysis, by a superstable protease, was a suitable strategy and an effective tool for analyzing intermediate structures of proteins with slow unfolding properties.

MATERIALS AND METHODS

Materials. GdnHCl was purchased from WAKO. All chemicals were of reagent grade.

Construction of Plasmids. Plasmids for the overexpression of Tk-RNase H2, Tm-RNase H2, and Tk-subtilisin were constructed as previously described.[25,29,30] Plasmids for the overexpression of mutant fragments 22 (residues 1–197), 20 (residues 1–176), 17 (residues 1–144), and 9 (residues 145–228) from Tk-RNase H2 were constructed from wild-type Tk-RNase H2 using standard recombinant DNA techniques.

Overproduction and Purification. Tk-RNase H2, Tm-RNase H2, and Tk-subtilisin were overproduced and purified as previously described.[25,29,30] Fragments 22, 20, 17, and 9 were overproduced and purified using the same methods that were used for Tk-RNase H2. Protein purity was analyzed by SDS–PAGE using a 15% polyacrylamide gel stained using Coomassie Brilliant Blue.[31] The concentrations of Tk-RNase H2, Tm-RNase H2, and Tk-subtilisin were estimated as previously described.[25,29,30] Protein concentrations were estimated by assuming absorbances at 280 nm of 0.3, 0.2, and 1.3 for 1 mg/mL fragments 20, 17, and 9, respectively. These values were calculated using extinction coefficients of 1576 M^{-1} cm^{-1} for Tyr and 5225 M^{-1} cm^{-1} for Trp at 280 nm.[32]

Measurement of CD Spectra. The CD spectra of all proteins in the absence and presence of GdnHCl were measured on a J-725 automatic spectropolarimeter (JASCO). The optical path length was 2 mm, and the protein concentration was 0.16 mg/mL. The buffer was 20 mM Tris-HCl (pH 9.0). All measurements were taken at 25 °C. To obtain the spectra of a refolded protein, the protein was completely unfolded in 4 M GdnHCl, diluted with buffer for refolding, and incubated at 25 °C until refolding reached

dx.doi.org/10.1021/bi300973n | *Biochemistry* 2012, 51, 9178–9191

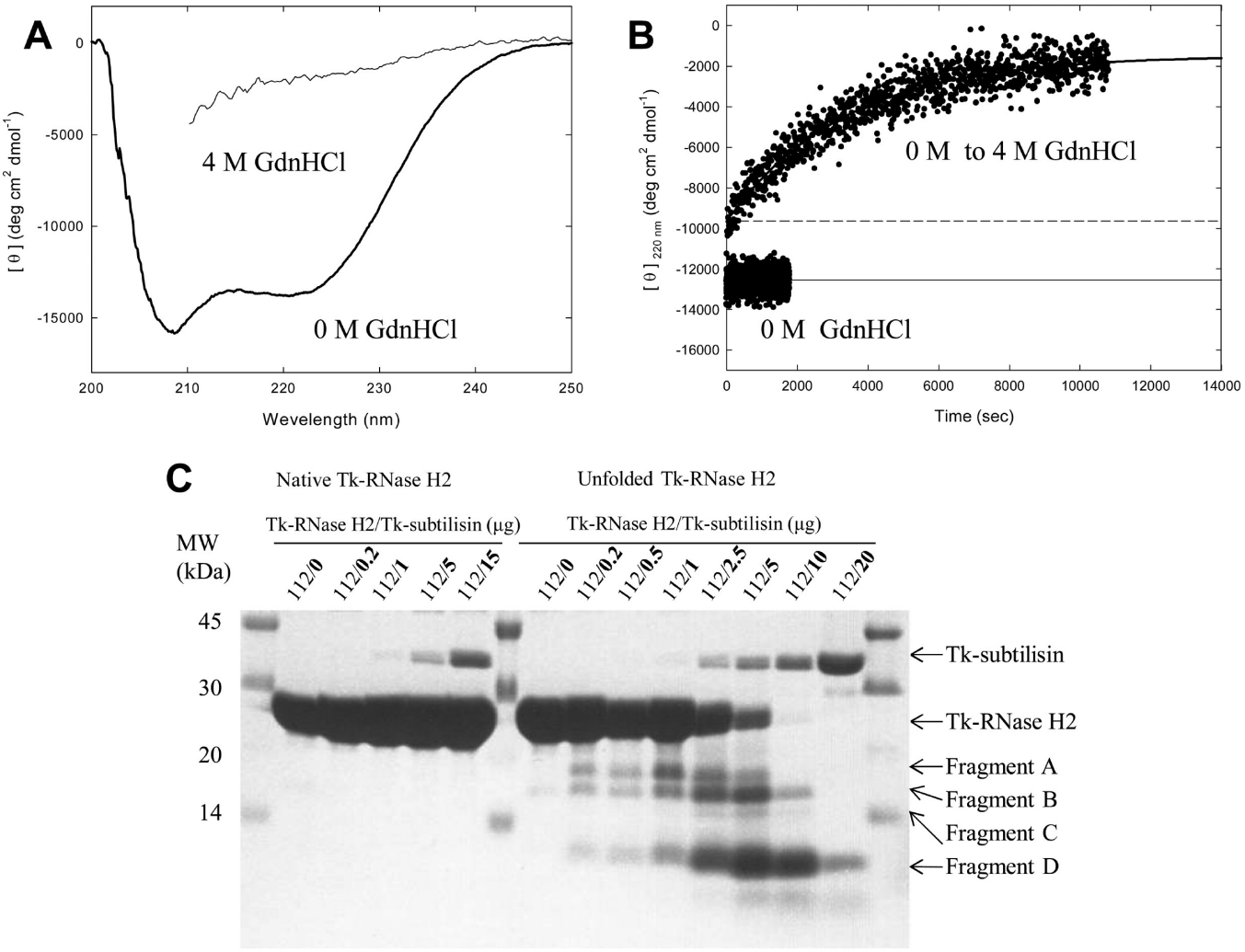

Figure 2. CD analysis and pulse proteolysis of native and unfolded states of Tk-RNase H2 at 25 °C. (A) Far-UV CD spectra of Tk-RNase H2 in the absence and presence of 4 M GdnHCl. (B) Native Tk-RNase H2 (0 M GdnHCl) was monitored by CD at 220 nm. Unfolding was initiated by rapid dilution of native Tk-RNase H2 under unfolding conditions (0−4 M GdnHCl) and monitored by CD at 220 nm. The thick line is a fit of the data to eq 1. The thin line shows the average signals in 0 M GdnHCl. The dashed line is the CD signal starting the slow phase. (C) Pulse proteolysis of the native and unfolded states of Tk-RNase H2 with Tk-subtilisin. Native Tk-RNase H2 (112 μg) and unfolded Tk-RNase H2 (112 μg) were dispensed into tubes. Proteolysis was performed via addition of Tk-subtilisin (0−20 μg) and incubation for 45 s. Proteolysis was quenched by 10% TCA, and products were quantified by tricine−SDS−PAGE. Bands corresponding to Tk-subtilisin, Tk-RNase H2, and cleavage products are indicated.

equilibrium. The mean residue ellipticity, θ, in units of degrees square centimeters per decimole, was calculated using an average amino acid molecular weight of 110.

Kinetic Experiments on GdnHCl-Induced Unfolding. Unfolding and refolding reactions were followed by a CD measurement at 220 nm as previously described.[25] The optical path length was 1 cm. The kinetic data were analyzed using eq 1:

$$A(t) - A(\infty) = \sum A_i e^{-k_i t} \quad (1)$$

where $A(t)$ is the value of the CD signal at a given time t, $A(\infty)$ is the value when no further change is observed, k_i is the apparent rate constant of the ith kinetic phase, and A_i is the amplitude of the ith phase. The GdnHCl concentration dependence of the logarithms of the apparent rate constant (k_{app}) for unfolding and refolding was also examined. The rate constants for unfolding and refolding in the absence of GdnHCl [$k_u(H_2O)$ and $k_r(H_2O)$, respectively] were calculated by fitting to eq 2:

$$\ln k_{app} = \ln[k_r(H_2O)\exp(-m_r[D]) + k_u(H_2O)\exp(-m_u[D])] \quad (2)$$

where [D] is the concentration of GdnHCl and m_u and m_r are the slopes of the linear correlations of ln k_u and ln k_r, respectively, with GdnHCl concentration. SigmaPlot was used for the fitting (SYSTAT). All kinetic experiments were performed in 20 mM Tris-HCl (pH 9.0). The protein concentration was 0.032−0.16 mg/mL.

Pulse Proteolysis of Native and Unfolded Proteins by Tk-Subtilisin. The basic pulse proteolysis procedure is shown in Figure 1A. Native proteins at 25 °C in 20 mM Tris-HCl (pH 9.0) and unfolded proteins in 20 mM Tris-HCl (pH 9.0) containing 4 M GdnHCl at 25 °C overnight were dispensed into reaction tubes (50 μL), and 2 μL of Tk-subtilisin at several concentrations in 10 mM acetate buffer (pH 5.0) was added to each aliquot. After 45 s, the reaction was quenched with 10% (w/v) TCA. Proteins were precipitated using 10% (w/v) TCA,

dx.doi.org/10.1021/bi300973n | Biochemistry 2012, 51, 9178−9191

washed with 70% acetone, and analyzed by 15% tricine−SDS−PAGE.[33]

Pulse Proteolysis of Kinetic Unfolding by Tk-Subtilisin. The basic procedure for unfolding studies by pulse proteolysis is shown in Figure 1B. The protein was unfolded in 20 mM Tris-HCl (pH 9.0) containing 4 M GdnHCl at 25 °C. Reaction mixtures were dispensed into aliquots (50 μL). At designated time points, 2 μL of Tk-subtilisin at several concentrations in 10 mM acetate buffer (pH 5.0) was added to each aliquot. After 45 s, the reaction was quenched and the proteins were precipitated and analyzed as described above.

N-Terminal Amino Acid Sequence and Molecular Mass Analysis. N-Terminal amino acid sequences of a protein were determined by a model 491 Procise automated sequencer (Applied Biosystems, Foster City, CA). The molecular mass of the protein was determined with matrix-assisted laser desorption ionization reflectron-type time-of-flight (MALDI-TOF) mass spectrometers, Autoflex and Ultraflex (Bruker Daltonik). Mass calibration was performed using protein calibration standard II. Bovine serum albumin (67 kDa), ovalbumin (44 kDa), chymotrypsinogen A (25 kDa), and RNase A (14 kDa) were used as standard proteins.

Heat-Induced Unfolding Experiments. Heat-induced unfolding was examined by CD monitoring at 220 nm. CD measurements were taken on a J-725 automatic spectropolarimeter as described previously.[25,29] The optical path length was 2 mm. The buffer was 20 mM Tris-HCl (pH 9.0). The protein concentration was 0.16 mg/mL. All experiments were performed at a scan rate of 1 °C/min. The mean molecular ellipticity, θ, in units of degrees square centimeters per decimole, was used. A nonlinear least-squares analysis[34] was used to fit the data to

$$y = (b_n + a_n[T] + (b_u + a_u[T]) \exp\{(\Delta H_m/RT)[(T - T_m)/T_m]\}) / (1 + \exp\{(\Delta H_m/RT)[(T - T_m)/T_m]\}) \quad (3)$$

where y is the observed CD signal at a given temperature T, b_n is the CD signal for the native state, b_u is the CD signal for the unfolded state, a_n is the slope of the pretransition of the baseline, a_u is the slope of the posttransition of the baseline, ΔH_m is the enthalpy of unfolding at the transition midpoint temperature (T_m), and R is the gas constant. Curve fitting was performed using SigmaPlot.

Anilino-8-naphthalenesulfonic Acid (ANS) Fluorescence Spectroscopy. ANS fluorescence spectroscopy was conducted on an RF-5300PC spectrofluorophotometer (Shimadzu). Binding of ANS (Sigma-Aldrich, St. Louis, MO) to proteins was analyzed by measuring the fluorescence of ANS at different temperatures. Protein (10 μM) and ANS (500 μM) were dissolved in 20 mM Tris-HCl (pH 9.0). Incubation was performed at different temperatures for 3 h prior to the measurement of ANS fluorescence. The excitation wavelength was 380 nm, and the emission was monitored from 400 to 600 nm. Spectra recorded in the absence of the protein were used as blanks.

Stability Curves. The $\Delta G(H_2O)$ values at each temperature were calculated from $k_u(H_2O)/k_r(H_2O)$. $\Delta G(H_2O)$ was plotted as a function of temperature, resulting in the stability profile of fragment 20. Stability curves obtained were fitted to the Gibbs−Helmholtz equation (eq 4):

$$\Delta G(H_2O) = \Delta H(T_o) - T\Delta S(T_o) + \Delta C_p [T - T_o - T \ln(T/T_o)] \quad (4)$$

where $\Delta H(T_o)$ and $\Delta S(T_o)$ are the enthalpy and entropy of unfolding at the reference temperature T_o, respectively. ΔC_p represents the difference in the heat capacity of the native and unfolded states.

RESULTS

The kinetics of GdnHCl-induced unfolding for Tk-RNase H2 were mainly examined at 50 °C, because the unfolding of Tk-RNase H2 is extremely slow at lower temperatures. We examined the kinetics of GdnHCl-induced unfolding of Tk-RNase H2 in more detail at 25 °C. Our results indicated that Tk-RNase H2 unfolded with multiple intermediates at moderate temperatures.

Unfolding of Tk-RNase H2 Examined by CD Spectroscopy. Far-UV CD spectra of Tk-RNase H2 were recorded in the absence and presence of 4 M GdnHCl at 25 °C. The spectra showed Tk-RNase H2 in the native and GdnHCl-unfolded states (Figure 2A).

The kinetics of GdnHCl-induced unfolding of Tk-RNase H2 were examined at 25 °C. The reaction was initiated by a jump to 4 M GdnHCl, and then the far-UV CD signal was recorded at 220 nm. The kinetic unfolding curve of Tk-RNase H2 is shown in Figure 2B. Tk-RNase H2 unfolded slowly, consistent with its slow unfolding property. At 25 °C, the unfolding was characterized by signal changes in the far-UV CD within dead times (~2 s). This indicated a burst phase in the kinetics of the slow unfolding of Tk-RNase H2. The burst phase, which was ~30% of the total signal changes between the unfolded and native states, was followed by a slower observable phase. The slow unfolding phase after the burst phase was approximated as a first-order reaction. The unfolding reaction was complete in ~4 h. The unfolding rate constant was 4.2×10^{-4} s^{-1} (Table 1).

Table 1. Unfolding Rate Constants (s^{-1}) of Tk-RNase H2 and Fragment 20 in 4 M GdnHCl

	10 °C	25 °C	50 °C	70 °C
Tk-RNase H2	5.7×10^{-4}	4.2×10^{-4}	4.2×10^{-3}	5.3×10^{-2}
fragment 20	5.9×10^{-4}	6.4×10^{-4}	3.7×10^{-3}	5.4×10^{-2}

Resistance of Tk-RNase H2 to Tk-Subtilisin. As shown in Figure 1A, we investigated whether Tk-RNase H2 could tolerate, or was degraded by Tk-subtilisin, in the absence (native state) and presence (unfolded state) of 4 M GdnHCl. The native and unfolded states of Tk-RNase H2 (112 μg) were digested by 0.2−15 and 0.2−20 μg of Tk-subtilisin, respectively, at 25 °C for 45 s. The samples were separated by tricine−SDS−PAGE, as shown in Figure 2C. The results showed that the native state of Tk-RNase H2 was not degraded by Tk-subtilisin under these conditions, because no reduction of the intact band and no cleavage products of Tk-RNase H2 were detected. At all tested amounts of Tk-subtilisin, the native state of Tk-RNase H2 was completely resistant to Tk-subtilisin. However, the unfolded state of Tk-RNase H2 (induced by 4 M GdnHCl) was degraded by Tk-subtilisin. Several cleavage products of Tk-RNase H2 appeared in the tricine−SDS−PAGE analysis. As the amount of Tk-subtilisin was increased (0.2−10 μg), more cleavage product bands formed. The bands of fragment A (17

dx.doi.org/10.1021/bi300973n | Biochemistry 2012, 51, 9178−9191

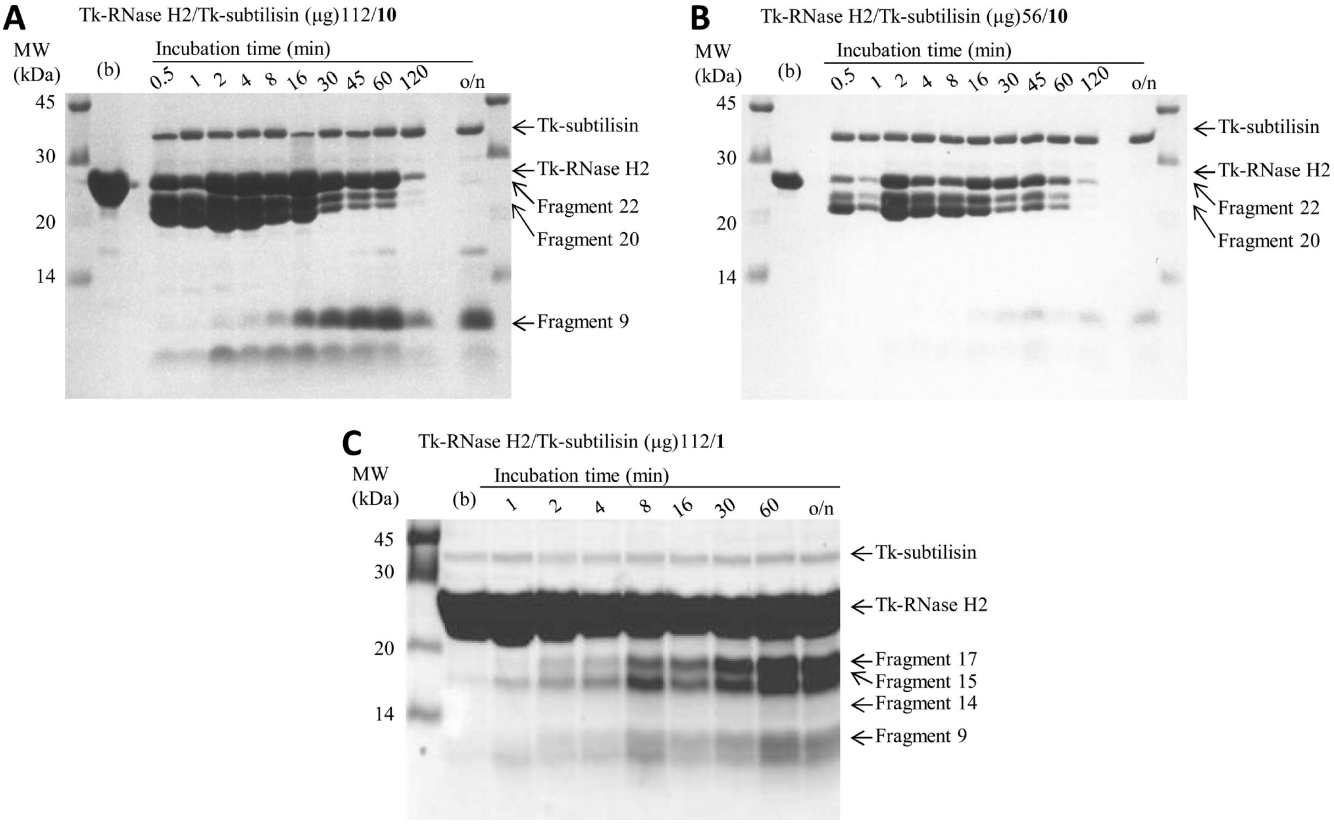

Figure 3. Pulse proteolysis of kinetic unfolding of Tk-RNase H2 by Tk-subtilisin under (A) condition 1, (B) condition 2, and (C) condition 3. Lanes (b) contained Tk-RNase H2 (112, 56, and 112 μg in panels A–C, respectively). Tk-RNase H2 was unfolded by adding 4 M GdnHCl. At each time point (0.5–120 min and overnight), the sample was dispensed into tubes, and proteolysis was performed via addition of Tk-subtilisin (10, 10, and 1 μg for panels A–C, respectively) and incubation for 45 s. Proteolysis was quenched by 10% TCA, and products were quantified by tricine–SDS–PAGE. Bands corresponding to Tk-subtilisin, Tk-RNase H2, and cleavage products are indicated.

kDa) and fragment B (15 kDa) were observed when Tk-RNase H2 was treated with 0.2 μg of Tk-subtilisin. With the addition of 2.5 μg of Tk-subtilisin, the bands of fragment C (14 kDa) and fragment D (9 kDa) also formed. These fragments could be regions of Tk-RNase H2 that did not completely unfold in 4 M GdnHCl.

The magnitudes of the four bands and the intact band of unfolded Tk-RNase H2 in 4 M GdnHCl were considerably reduced in tricine–SDS–PAGE gels by the addition of larger amounts of Tk-subtilisin (>20 μg). In particular, the intact band of full-length Tk-RNase H2 that was unfolded in 4 M GdnHCl disappeared with the addition of 10 μg of Tk-subtilisin. The result indicated that Tk-subtilisin still retained its polypeptide digesting activity in the presence of 4 M GdnHCl and that Tk-RNase H2 was nearly completely degraded in its unfolded state by large amounts of Tk-subtilisin. The robustness of Tk-RNase H2 and Tk-subtilisin makes them good target proteins and proteases for pulse proteolysis experiments, because the native state of Tk-RNase H2 was resistant to Tk-subtilisin, but complete digestion of the unfolded state of Tk-RNase H2 was achieved by the addition of Tk-subtilisin.

Observation of the Kinetic Unfolding Intermediates of Tk-RNase H2 by Pulse Proteolysis. Unfolding experiments using pulse proteolysis have examined proteins from mesophilic bacteria (*Escherichia coli* RNase H1, *E. coli* maltose binding protein, etc.) using a mesophilic protease as previously conducted by Park and Marqusee,[35] Na and Park,[36] Chang and Park,[37] and Kim et al.[38] In this study, pulse proteolysis experiments were performed according to the scheme in Figure 1B, which was designed using the results of the unfolding property of Tk-RNase H2 in 4 M GdnHCl and the resistance of the native state of Tk-RNase H2 to Tk-subtilisin. To identify the kinetic unfolding intermediates of Tk-RNase H2, its native state needed to be completely resistant to Tk-subtilisin while its unfolded state needed to be degradable.

As the stability of GdnHCl and the tolerance of Tk-RNase H2 kinetic unfolding intermediates to Tk-subtilisin were not known, we used three conditions with different ratios of Tk-RNase H2 to Tk-subtilisin. In the first and second conditions, the amounts of Tk-RNase H2 differed (112 μg in condition 1 and 56 μg in condition 2), although the amount of Tk-subtilisin was the same (10 μg). In the third condition, the amount of Tk-subtilisin was smaller (1 μg) and the amount of Tk-RNase H2 was the same as the amount in condition 1 (112 μg). Unfolding of Tk-RNase H2 was initiated by the addition of 4 M GdnHCl. At designated time points, 10 μg of Tk-subtilisin was added to 112 μg of Tk-RNase H2 under condition 1 and to 56 μg of Tk-RNase H2 under condition 2. Under condition 3, 1 μg of Tk-subtilisin was added to 112 μg of Tk-RNase H2. After incubation for 45 s, the reaction was terminated with trichloroacetic acid (TCA). The remaining intact Tk-RNase H2 and its degradation products were detected by tricine–SDS–PAGE, as shown in panels A (condition 1), B (condition 2), and C (condition 3) of Figure 3.

In panels A and B of Figure 3, an intact band and several cleavage products of Tk-RNase H2 were observed. These results differed from previous reports,[35–38] in which the band intensities of the intact proteins gradually disappeared over

dx.doi.org/10.1021/bi300973n | *Biochemistry* 2012, 51, 9178–9191

Table 2. Fragments of Tk-RNase H2 Produced by Tk-Subtilisin Digestion

		N-terminal analysis			possible region in Tk-RNase H2	
	tricine–SDS–PAGE (kDa)	N-terminal sequence	sequence in Tk-RNase H2	measured mass (Da)	theoretical mass (Da)	residues
Tk-RNase H2	26	–	–	25780	25799	1–228
fragment 22	22	MKIA	$M_1K_2I_3A_4$	21969	22007	1–197
fragment 20	20	MKIA	$M_1K_2I_3A_4$	19596	19603	1–177
fragment 17	17	MKIA	$M_1K_2I_3A_4$	15885	15899	1–144
fragment 15	15	AVVV	$A_{21}V_{22}V_{23}V_{24}$	13800	13784	21–144
fragment 14	14	DVDE	$D_{108}V_{109}D_{110}E_{111}$	–	14073	108–228
fragment 9	9	SLIA	$S_{145}L_{146}I_{147}A_{148}$	–	9917	145–228

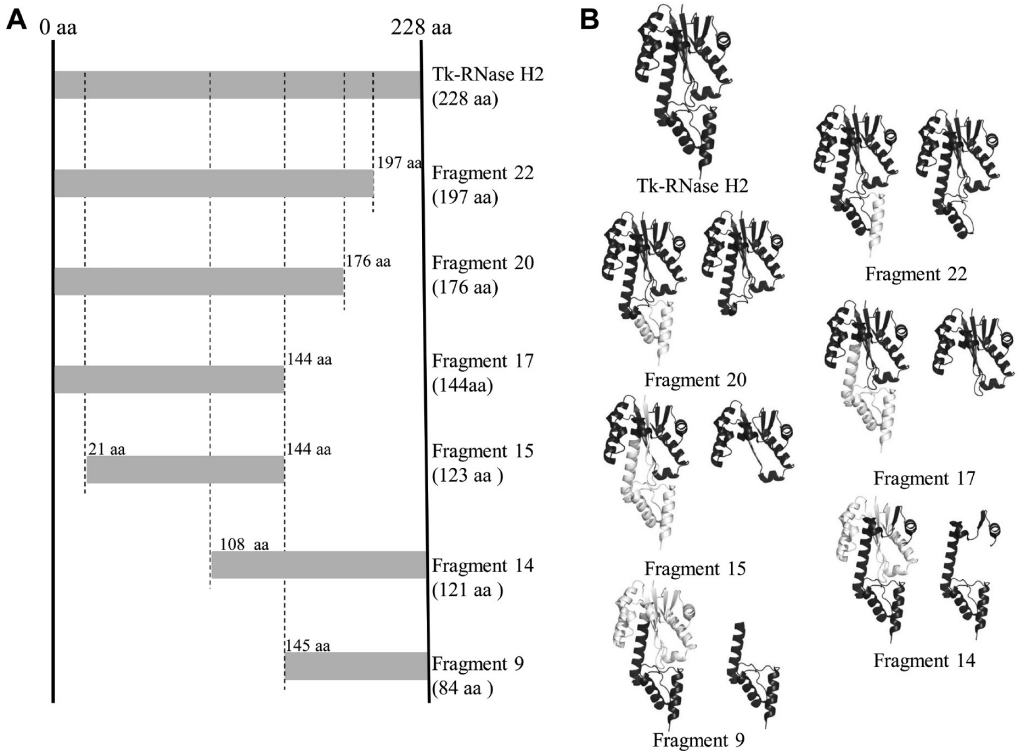

Figure 4. Schematic illustration of cleavage products from pulse proteolysis. (A) Schematic diagrams of Tk-RNase H2, fragment 22, fragment 20, fragment 17, fragment 15, fragment 14, and fragment 9. (B) Structures of Tk-RNase H2 (PDB entry 1IO2) and models of fragments. In fragment structures, the left structure represents the whole structure with the deleted region (gray) and the right structure represents the corresponding region.

time and the other bands did not appear, indicating a two-state unfolding process.

In our experiments, although native Tk-RNase H2 was completely resistant to Tk-subtilisin in 4 M GdnHCl, the magnitude of the intact band decreased by more than half in 0.5 min. Two heavy chain fragments (fragments 22 and 20) at ~20 kDa appeared. Moreover, the amount of the intact protein at 0.5 and 1 min was smallers than that at 2–16 min. This did not originate from the overloading of sample in tricine–SDS–PAGE or a lower efficiency of precipitation, because the smaller amounts of samples in tricine–SDS–PAGE showed similar results and there was no reduction detected in the magnitude of the intact band in the experiments without Tk-subtilisin (data not shown). These results suggested that some intact proteins were in a digested form in the early stage of unfolding, changing to a form resistant to Tk-subtilisin during the unfolding in GdnHCl (see Discussion). At 120 min, only a faint band of the intact protein was observed. The Tk-subtilisin resistant form of Tk-RNase H2 was gradually unfolded by the denaturant and then degraded by Tk-subtilisin.

In Figure 3A, a 9 kDa light chain fragment (fragment 9) gradually appeared over time. Only a faint band of fragment 9 was seen in Figure 3B, in which a smaller amount of Tk-RNase H2 was treated with Tk-subtilisin, while fragments 20 and 22 appeared under condition 2, similar to condition 1. This suggested that during the slow unfolding of Tk-RNase H2, fragment 9 accumulated from the Tk-subtilisin resistant form but the structure of fragment 9 was less resistant to Tk-subtilisin than fragments 20 and 22.

Using smaller amounts of Tk-subtilisin (condition 3), several degraded fragments (fragments 17, 15, 14, and 9) and a large amount of intact Tk-RNase H2 were observed (Figure 3C). These fragments appeared gradually over time. The molecular masses of fragments 17, 15, 14, and 9 closely resembled those of fragments A–D, respectively, in Figure 2C. The regions of Tk-RNase H2 that did not completely unfold in 4 M GdnHCl might correspond to the residual structures of Tk-RNase H2 during the unfolding process that are tolerant to Tk-subtilisin.

Identification of the Cleavage Sites in Tk-RNase H2 by Pulse Proteolysis. When Tk-RNase H2 was digested with Tk-

dx.doi.org/10.1021/bi300973n | *Biochemistry* 2012, 51, 9178–9191

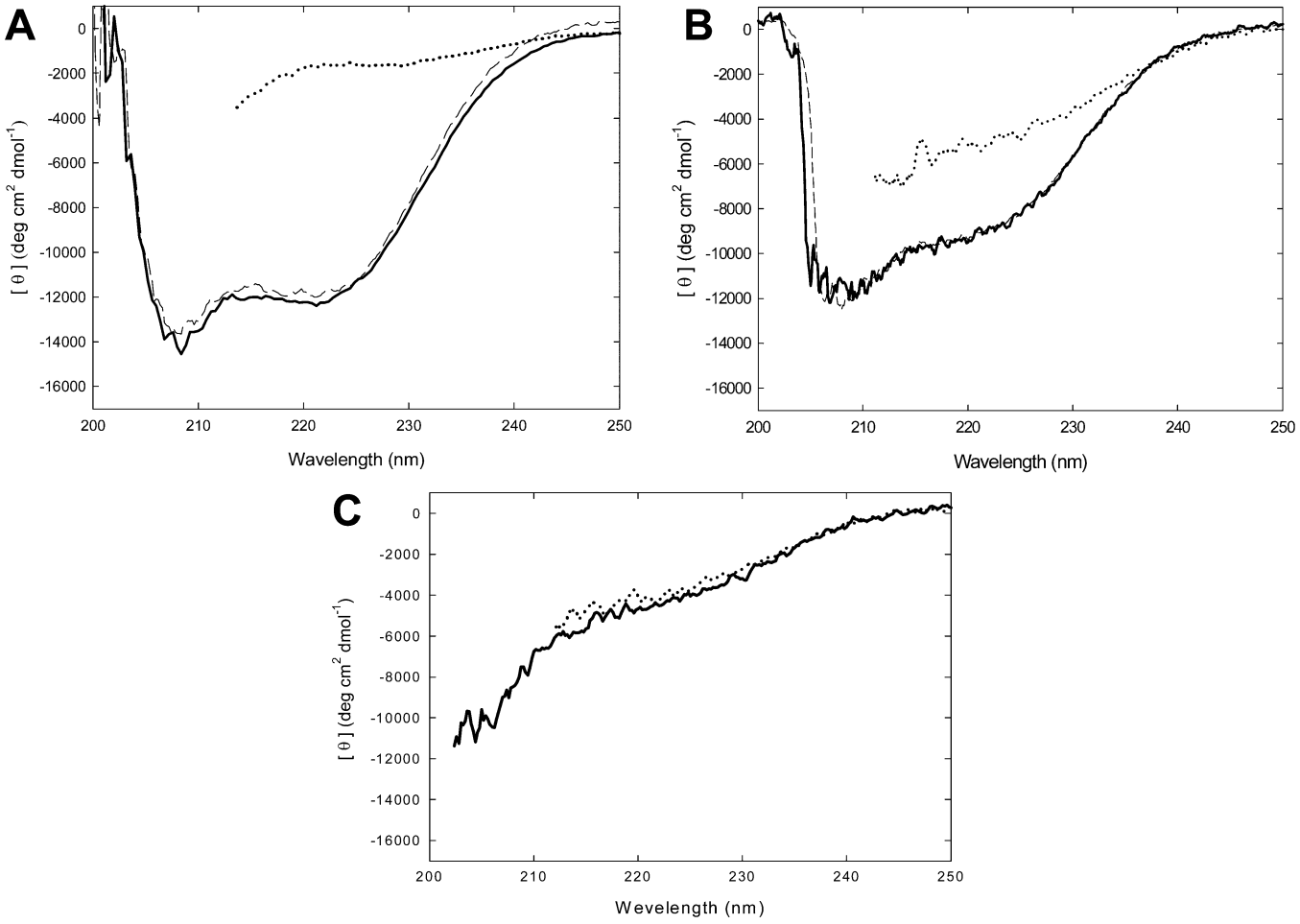

Figure 5. Far-UV CD spectra of fragments of Tk-RNase H2 in the absence (—) and presence (···) of 4 M GdnHCl at 25 °C. (A) Fragment 20. The dashed line is the spectrum of the refolded protein in the presence of 1 M GdnHCl. (B) Fragment 9. The dashed line is the spectrum of the refolded protein in the presence of 1 M GdnHCl. (C) Fragment 17.

subtilisin during unfolding, six fragments (fragments 22, 20, 17, 15, 14, and 9) were observed on tricine−SDS−PAGE gels (Figure 3A−C). To identify these fragments by N-terminal sequencing, Tk-RNase H2 was digested by Tk-subtilisin, separated by tricine−SDS−PAGE, and blotted onto PVDF membranes. Sequencing the fragments by Edman degradation resulted in four sequences: MKIA, AVVV, DVDE, and SLIA, corresponding to residues 1−4, 21−24, 108−111, and 145−148 of Tk-RNase H2, respectively (Table 2). These results showed that fragments 22, 20, and 17 were degraded only in the C-terminal region of Tk-RNase H2. We also analyzed the proteolytic products by MALDI-TOF mass spectrometry (MS). The measured value, 25780 Da, of Tk-RNase H2 in the presence of 4 M GdnHCl was slightly different from the theoretical value, 25799 Da. This might have been affected by the GdnHCl. The molecular masses of fragments 22, 20, 17, and 15 of Tk-RNase H2 in 4 M GdnHCl were 21969, 19596, 15885, and 13800 Da, respectively. Therefore, the possible regions of fragments 22, 20, 17, and 15 were estimated to be residues 1−197, 1−176, 1−144, and 21−144 of Tk-RNase H2, respectively (Table 2 and Figure 4A). The possible region of fragments 14 and 9 was estimated by tricine−SDS−PAGE and N-terminal sequencing because the fragments did not crystallize well on the MALDI-TOF MS plate. The results showed that fragments 14 and 9 were located approximately at residues 108−228 and 145−228 of Tk-RNase H2, respectively (Table 2 and Figure 4A). Figure 4B shows simple tertiary structural models from the crystal structure of Tk-RNase H2 [Protein Data Bank (PDB) entry 1IO2]. Fragments 22, 20, and 17 have lost their C-terminal regions. Fragment 15 has lost both its C-terminal and N-terminal regions. Fragments 14 and 9 might include the C-terminal regions.

Construction of Tk-RNase H2 Unfolding Intermediate Mimics and Their CD Spectroscopy. Kinetic unfolding intermediate mimics of Tk-RNase H2 were constructed using protein engineering. We successfully obtained three polypeptides, corresponding to fragments 20, 17, and 9. The remaining polypeptide fragments were not overexpressed in *E. coli*. The far-UV CD spectra of Tk-RNase H2 and fragments 20, 17, and 9 were recorded in the absence and presence of 4 M GdnHCl at 25 °C (Figure 5). The spectra under the folded conditions obtained from the unfolded states by dilution of GdnHCl were also measured. The far-UV CD spectra of fragment 17 were the same under the native and unfolded conditions and represented an unfolded conformation indicating that fragment 17 did not form any secondary structure in the absence of GdnHCl (Figure 5C). The far-UV CD spectra were different for the native and unfolded conditions of Tk-RNase H2 and fragments 20 and 9 (Figures 2A and 5A,B). These spectra under the native condition showed characteristics of secondary structure. The GdnHCl-induced unfolding of fragments 20 and 9 was almost reversible. The far-UV CD spectra of Tk-RNase H2 and

dx.doi.org/10.1021/bi300973n | *Biochemistry* 2012, 51, 9178−9191

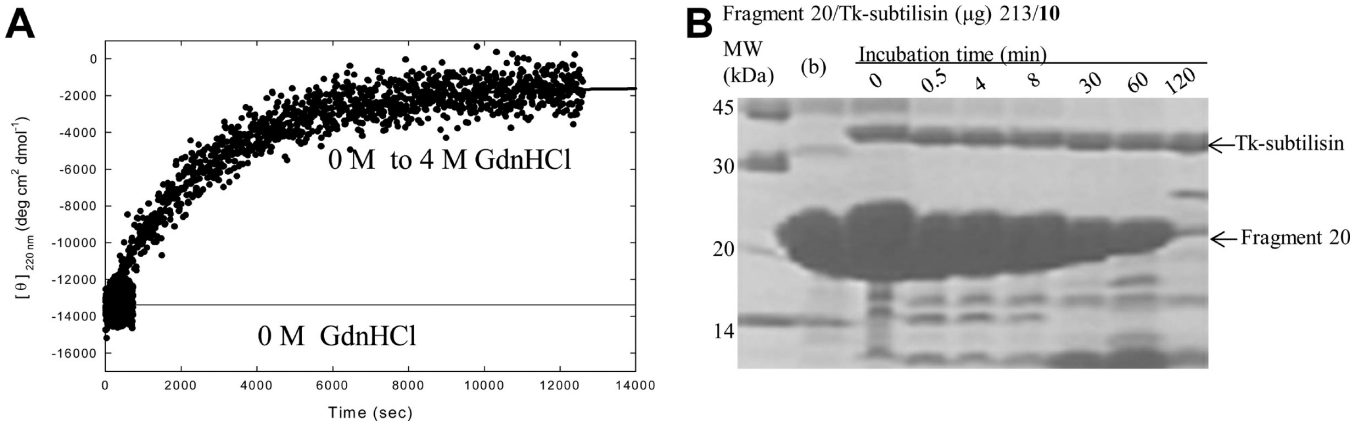

Figure 6. Kinetic unfolding curve and pulse proteolysis of fragment 20 at 25 °C. (A) The native state of fragment 20 (0 M GdnHCl) was monitored by CD at 220 nm. Unfolding was initiated by rapid dilution of native fragment 20 into unfolding conditions (0−4 M GdnHCl) and monitored by CD at 220 nm: (thin line) average signals in 0 M GdnHCl and (thick line) a fit of the data to eq 1. (B) Pulse proteolysis in kinetic unfolding of fragment 20 by Tk-subtilisin. Lane (b) represents native fragment 20 (218 μg). Fragment 20 (218 μg) was unfolded by addition ofg 4 M GdnHCl. At each time point (0−120 min), the sample was dispensed into a tube, and proteolysis was performed via addition of Tk-subtilisin (10 μg) and incubation for 45 s. Bands corresponding to Tk-subtilisin and fragment 20 are indicated.

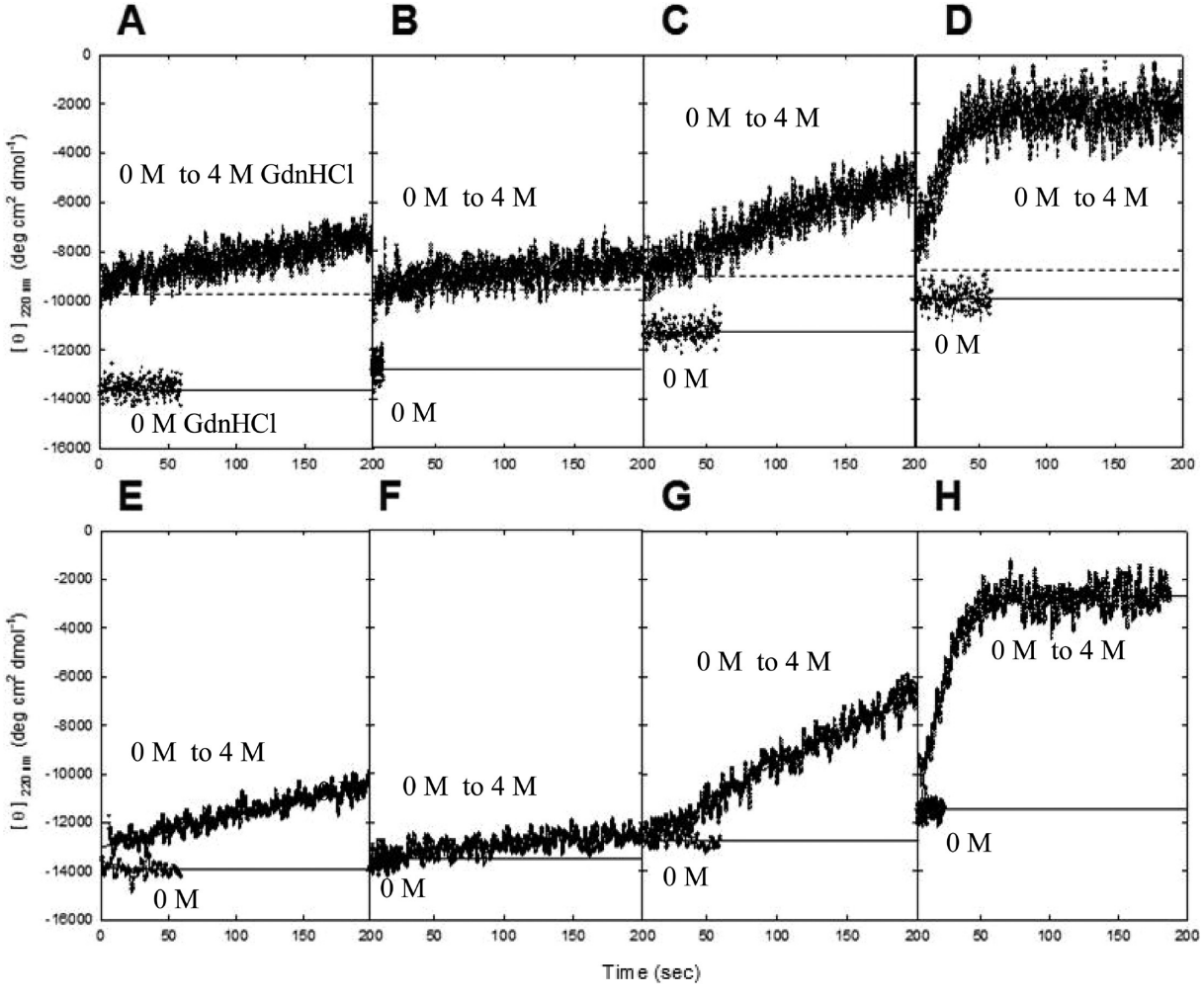

Figure 7. Kinetic unfolding curves of Tk-RNase H2 and fragment 20 at several temperatures. Native states of Tk-RNase H2 (A−D) and fragment 20 (E−H) (0 M GdnHCl) were monitored by CD at 220 nm. Unfolding was initiated by rapid dilution of native Tk-RNase H2 (A−D) and fragment 20 (E−H) into unfolding conditions (0−4 M GdnHCl) and monitored by CD at 220 nm at 10 (A and E), 25 (B and F), 50 (C and G), and 70 °C (D and H). Thin lines show average signals in 0 M GdnHCl. Thick lines show fits of the data to eq 1. Dashed lines shows CD signals starting the slow phase.

dx.doi.org/10.1021/bi300973n | *Biochemistry* 2012, 51, 9178−9191

fragment 20 produced very similar signals (Figures 2A and 5A), suggesting that the secondary structure of fragment 20 resembled that of Tk-RNase H2.

Kinetic Study of Fragment 9. To determine if fragment 9, observed in the proteolysis experiments, was a robust intermediate form, we examined the kinetics of GdnHCl-induced unfolding of fragment 9 at 25 °C. We detected a significant loss of CD value in the dead time (2 s) of the experiments when kinetic unfolding was measured at 25 °C (data not shown). This result indicated that fragment 9 unfolded quite rapidly (<2 s) and therefore was not a robust intermediate form in the unfolding of Tk-RNase H2. Panels A and B of Figure 3 show the bands of fragment 9 on a tricine–SDS–PAGE gel, and the bands of fragment D that probably corresponds to fragment 9 are shown in Figure 2A. These results suggest that fragment 9 has a Tk-subtilisin resistant structure but no robust native structure.

Characterization of Fragment 20 by Kinetic Unfolding and Pulse Proteolysis. The kinetics of GdnHCl-induced unfolding of fragment 20 were examined at 25 °C. The kinetic unfolding curve is shown in Figure 6A. Fragment 20 unfolded slowly. Of note is the fact that the burst phase signal was not detected in its kinetic curves. The kinetic trace was approximated to a first-order reaction. The result showed that the unfolding rate constant of fragment 20 (6.4×10^{-4} s^{-1}) was equal to that of Tk-RNase H2 (4.2×10^{-4} s^{-1}) after the burst phase at 25 °C (Table 1).

The native state of fragment 20 (213 μg) was largely undegraded by 10 μg of Tk-subtilisin (Figure 6B, lane 0). However, fragment 20 (213 μg) in the presence of 4 M GdnHCl was degraded by 10 μg of Tk-subtilisin after 120 min (Figure 6B, lane 120). For pulse proteolysis, the unfolding of fragment 20 was initiated by the addition of 4 M GdnHCl. At designated time points, 10 μg of Tk-subtilisin was added to 213 μg of fragment 20. The amount of remaining intact fragment 20 and its degradation products were detected. Figure 6B shows that the magnitude of the intact band decreased over time, but few degradation products were detected. This result was similar to previous reports.[35−38] During the unfolding, fragment 20 appeared to lose resistance to Tk-subtilisin.

The change in far-UV CD signals in GdnHCl-induced unfolding and proteolysis experiments clearly indicated a two-state unfolding process for fragment 20. The unfolding speed of fragment 20 was similar with the slow unfolding speed after the burst phase of Tk-RNase H2 (Table 1). These results suggested that fragment 20 is a rate-limiting factor in the slow overall unfolding process of Tk-RNase H2.

Relationship between the Temperature and the Unfolding Property. To observe the relationship between the temperature and the unfolding process of Tk-RNase H2 and fragment 20 by kinetic analysis, we initiated the unfolding reaction by a jump to 4 M GdnHCl followed by measurement of far-UV CD signals at 10, 25, 50, and 70 °C. At each temperature, the unfolding of Tk-RNase H2 was characterized by signal changes in the far-UV CD spectra within the dead time (~2 s) (Figure 7A–D). This indicated burst phases in the slow kinetic unfolding process of Tk-RNase H2 at each temperature. Burst phases at 10, 25, 50, and 70 °C were ~40, ~30, ~20, and 5%, respectively, of the total signal changes between the unfolded and native states. These were followed by slower phases. However, we could not detect the burst phase signals in the kinetic curves of fragment 20 at all the temperatures investigated (Figure 7E–H). The unfolding rates after the burst phase of Tk-RNase H2 were the same as the unfolding rates of fragment 20 at each temperature (Table 1). This indicates that the unfolding speeds of fragment 20 were similar with the slow unfolding speeds after the burst phase of Tk-RNase H2 at each temperature. This result suggested that fragment 20 was a rate-limiting factor in the slow unfolding of the overall structure of Tk-RNase H2 at each temperature. Furthermore, the native state signal points of Tk-RNase H2 were affected by temperature to a greater extent than the signal points for fragment 20 and the signal points starting the slow phase of Tk-RNase H2. This indicates that the amount of Tk-RNase H2 not involved in slow unfolding was influenced by the change in temperature.

Heat-Induced Unfolding of Tk-RNase H2 and Fragment 20. The thermal unfolding property of Tk-RNase H2 was compared to that of fragment 20. A change in the far-UV CD signal at 220 nm was used to detect the heat-induced unfolding of Tk-RNase H2 and fragment 20. Figure 8 shows

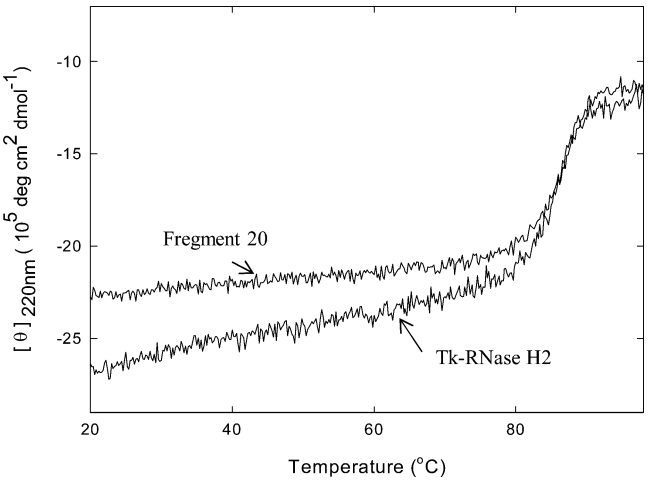

Figure 8. Heat-induced unfolding curve of Tk-RNase H2 and fragment 20, monitored by CD at 220 nm.

representative heat-induced unfolding curves for Tk-RNase H2 and fragment 20. Heat-induced unfolding of fragment 20 was highly reversible and exhibited a two-state transition. The unfolding curve was fit to eq 3 to obtain the T_m. The T_m for fragment 20 was estimated to be 86.8 °C, which was comparable to that of Tk-RNase H2 (85.7 °C). The slope of the baseline before the phase transition was different between the Tk-RNase H2 and fragment 20, as shown by far-UV CD signal changes (Figure 8). This difference resulted from the C-terminal region of Tk-RNase H2, which was deleted in fragment 20. These results demonstrated a structural change in the C-terminal region of Tk-RNase H2 during heat-induced unfolding prior to the phase transition.

Anilino-8-naphthalenesulfonic Acid (ANS) Binding of Tk-RNase H2 and Fragment 20. To obtain more information about the heat-induced conformational change of Tk-RNase H2, we analyzed Tk-RNase H2 and fragment 20 by their ability to bind ANS. ANS binds effectively to the hydrophobic surfaces of proteins.[39,40] Panels A and B of Figure S1 of the Supporting Information show that the maximal ANS fluorescence of Tk-RNase H2 occurred at 10 °C, and ANS fluorescence was reduced with an increase in temperature. The ANS fluorescence with fragment 20 was much lower than with Tk-RNase H2 at all temperatures. These results suggested that

dx.doi.org/10.1021/bi300973n | Biochemistry 2012, 51, 9178–9191

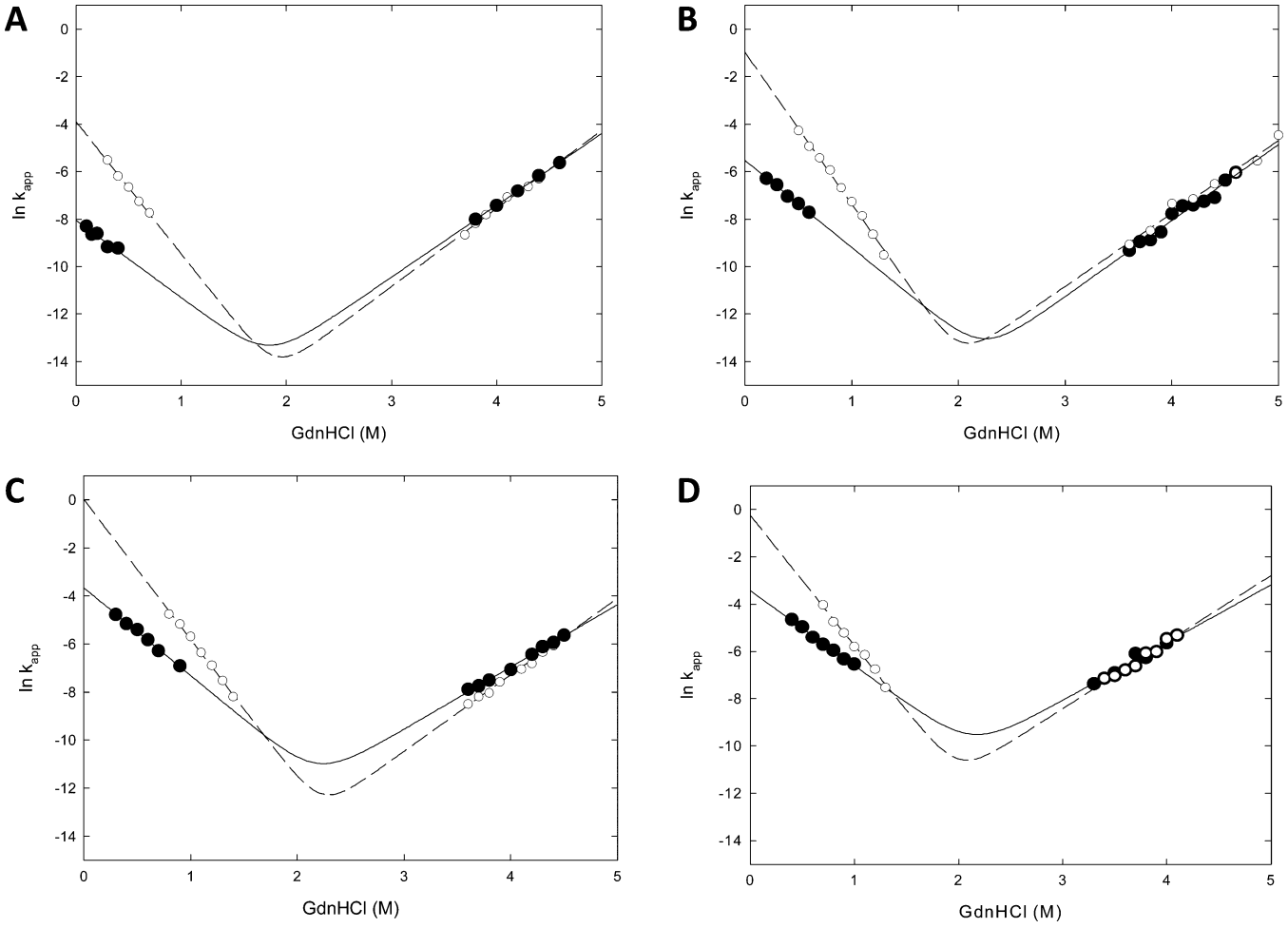

Figure 9. Kinetics of unfolding and refolding of Tk-RNase H2 and fragment 20 at several temperatures. GdnHCl concentration dependence of the logarithm of the apparent rate constant (k_{app}) of unfolding and refolding kinetics of Tk-RNase H2 (○) and fragment 20 (●) at 15 (A), 25 (B), 40 (C), and 50 °C (D). Dashed (Tk-RNase H2) and solid (fragment 20) lines are the best fits to eq 2.

Table 3. Kinetic Parameters of Unfolding and Refolding of Tk-RNase H2 and Fragment 20

	Tk-RNase H2					fragment 20				
temp (°C)	$k_u(H_2O)$ (s^{-1})	m_u (M^{-1} s^{-1})	$k_r(H_2O)$ (s^{-1})	m_r (M^{-1} s^{-1})	$\Delta G(H_2O)$ (kJ mol^{-1})	$k_u(H_2O)$ (s^{-1})	m_u (M^{-1} s^{-1})	$k_r(H_2O)$ (s^{-1})	m_r (M^{-1} s^{-1})	$\Delta G(H_2O)$ (kJ mol^{-1})
15	4.12×10^{-9}	3.2	0.0205	−5.5	36.5	3.31×10^{-9}	3.0	0.0003	−3.1	30.0
25	6.02×10^{-10}	3.3	0.38	−6.2	50.2	1.74×10^{-9}	3.0	0.003	−4.2	35.2
40	2.00×10^{-9}	3.1	1.01	−5.8	51.0	2.96×10^{-8}	2.6	0.0257	−3.6	35.0
50	5.0×10^{-8}	2.8	0.78	−5.0	44.5	2.04×10^{-7}	2.5	0.0323	−3.2	32.0

the hydrophobic surface of Tk-RNase H2 was larger at the lower temperature and decreased with an increase in temperature. However, fragment 20 maintained a small hydrophobic surface at each temperature. As fragment 20 is a C-terminal deletion mutant of Tk-RNase H2, this difference was attributed to the C-terminal region of Tk-RNase H2. These results demonstrated that the conformational change of the C-terminal region of Tk-RNase H2 with the increase in temperature was combined with a large hydrophobic surface change.

Kinetic Parameters of Fragment 20. To quantitatively evaluate the kinetic folding and unfolding parameters of Tk-RNase H2 and fragment 20, the kinetics of GdnHCl-induced unfolding and refolding were measured between 15 and 50 °C. Kinetic curves of fragment 20 for unfolding and folding are shown in panels A and B of Figure S2 of the Supporting Information. All kinetic traces of fragment 20 and the slow phase of Tk-RNase H2 were approximated as first-order reactions. The GdnHCl concentration dependence on logarithms of the apparent rate constant (k_{app}) of the unfolding and folding kinetics of fragment 20 and the slow phase of Tk-RNase H2 at various temperatures is shown in Figure 9. The kinetic parameters were estimated by extrapolation to 0 M GdnHCl using eq 2, and parameters for unfolding and refolding of Tk-RNase H2 and fragment 20 at different temperatures are listed in Table 3. The $\Delta G(H_2O)$ value at each temperature for fragment 20 was evaluated from $k_u(H_2O)/k_r(H_2O)$. The rates of unfolding of fragment 20 were comparable to the rates of slow unfolding after the burst phase of Tk-RNase H2. These results suggested that the unfolding reaction of fragment 20 was rate-limiting in the slow unfolding process of Tk-RNase H2 at each temperature. However, the rates of refolding of fragment 20 were different from those of Tk-RNase H2 at all

dx.doi.org/10.1021/bi300973n | *Biochemistry* 2012, 51, 9178−9191

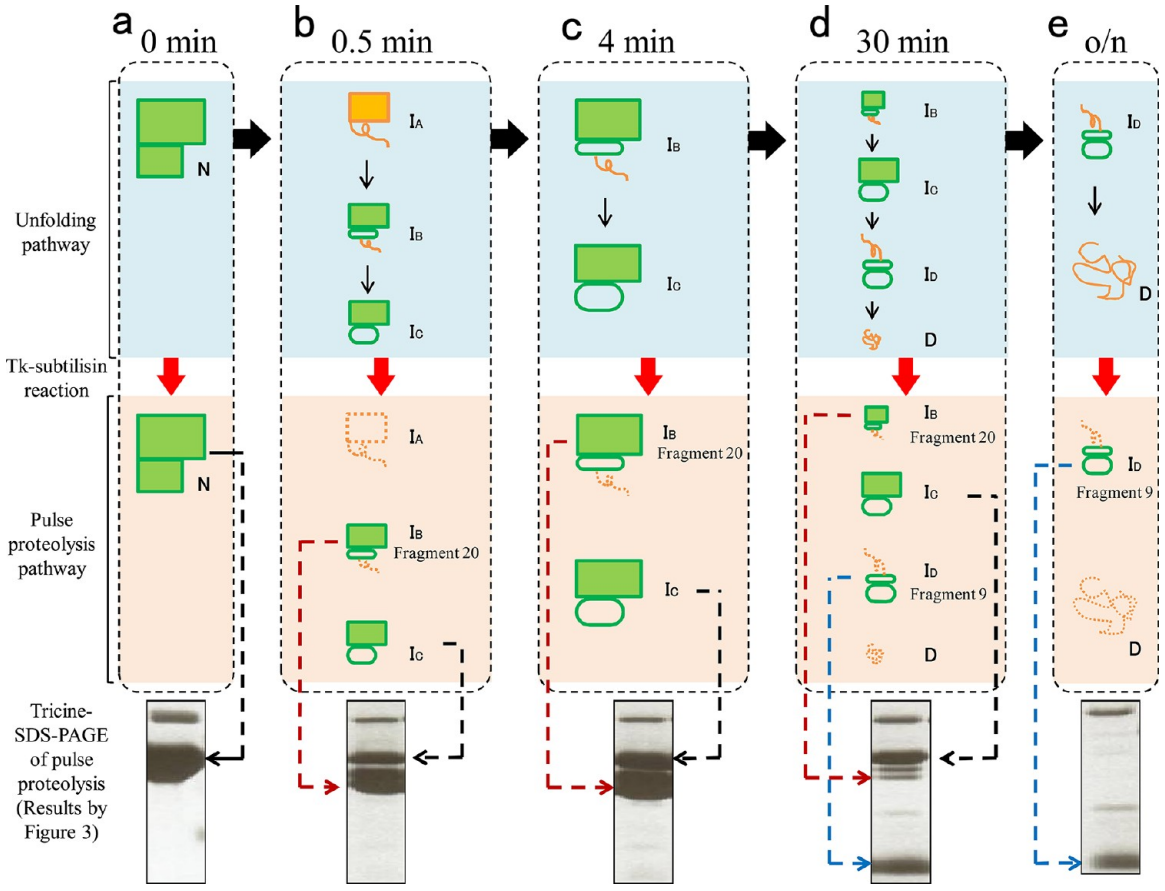

Figure 10. Unfolding pathway (blue background) and pulse proteolysis pathway (red background) illustrated on each time scale (a–e). Red arrows denote reactions by Tk-subtilisin. Black arrows denote shifts in the unfolding pathway. Results of tricine–SDS–PAGE for the pulse proteolysis pathway are connected by dashed arrows. In each state, the size represents their abundance ratio on each time scale (a–e). Rectangles are regions with secondary structures. Ellipses are regions with some structures but no secondary structures. Curves are regions without folded structures. The Tk-subtilisin resistant form is colored green and the digested form orange.

temperatures. Therefore, fragment 20 refolded more slowly than Tk-RNase H2.

$\Delta G(H_2O)$ was plotted as a function of temperature, resulting in the stability profile of fragment 20 shown in Figure S3 of the Supporting Information. The stability profile displayed a maximal $\Delta G(H_2O)$ at ~30 °C and was fit to a two-state model generated by eq 4. Tk-RNase H2 was more stable than fragment 20. These results indicated that the C-terminal region of Tk-RNase H2 stabilized the protein at moderate temperatures and contributed to the folding, but not to the slow unfolding, of Tk-RNase H2.

Unfolding Properties of Tm-RNase H2 Determined by Kinetic Study and Pulse Proteolysis. In our previous work, the slow unfolding rates of Tk-RNase H2 and Tm-RNase H2 were examined in the presence of ~4 M GdnHCl.[29] Via extrapolation of the unfolding rate constants to 0 M GdnHCl at 25 °C, Tk-RNase H2 showed slow unfolding, but this was not observed with Tm-RNase. To confirm this result, we conducted a kinetic and pulse proteolysis study of Tm-RNase H2.

The kinetics of GdnHCl-induced unfolding of Tm-RNase H2 were examined at 25 °C. Tm-RNase H2 unfolded slowly in 4 M GdnHCl (Figure S4A of the Supporting Information). The kinetic trace was approximated as a first-order reaction. The native formation of Tm-RNase H2 (112 μg) was not degraded by 10 μg of Tk-subtilisin (Figure S4B of the Supporting Information, lane 0). However, Tm-RNase H2 (112 μg) was unfolded by 4 M GdnHCl at 120 min and was mostly degraded by 10 μg of Tk-subtilisin (Figure S4B of the Supporting Information, lane 120). For pulse proteolysis, degradation products were detected by tricine–SDS–PAGE. As shown in Figure S4B of the Supporting Information, the magnitude of the intact band decreased over time. No fragments corresponded to fragments 22 and 20 in panels A and B of Figure 3. The proteolysis experiments showed clearly the two-state unfolding process of Tm-RNase H2. Although the unfolding rate of Tm-RNase H2 was slow in 4 M GdnHCl, as observed in Tk-RNase H2, Tm-RNase H2 showed a two-state unfolding process in pulse proteolysis experiments, unlike Tk-RNase H2. This result suggested that Tk-RNase H2 and Tm-RNase H2 have different unfolding mechanisms.

■ DISCUSSION

Intermediate States in the Unfolding of Tk-RNase H2. Pulse proteolysis experiments with Tk-RNase H2 showed that the magnitude of the intact band of the protein was reduced by more than half, and the presence of large amounts of the bands representing fragments 20 and 22 developed at the early time points (Figure 3A,B). However, the native state of Tk-RNase H2 was completely resistant to Tk-subtilisin. The amounts of intact protein and fragments 20 and 22 at the early incubation time of 0.5 min were smaller than those at the intermediate incubation time of 2–16 min (Figure 3A,B). This was not seen

dx.doi.org/10.1021/bi300973n | Biochemistry 2012, 51, 9178–9191

by pulse proteolysis in the unfolding process of any other proteins, including fragment 20 or Tm-RNase H2 (Figure 6B, Figure S4B of the Supporting Information, and previous reports[35−38]). This suggested a digested form (I_A-state) in the early stage of unfolding, changing to a partially digested form (I_B-state) and a from resistant to Tk-subtilisin (I_C-state) during unfolding in GdnHCl. These intermediates had structural changes in the C-terminal region. This was confirmed by subsequent experiments.

Fragment 20 had lost the C-terminal region of Tk-RNase H2, where two α-helices are located (Figure 4). The characterization of this fragment showed that proteolysis experiments indicated a clear two-state unfolding process (Figure 6B). The burst phase signal of kinetic unfolding was not detected in fragment 20 (Figure 6A). The unfolding speeds of fragment 20 were similar to the unfolding speeds of the slow phases of Tk-RNase H2 at each temperature (Table 1). The results suggest that the I_A-state lost the secondary structure of the C-terminus, resulting in the degradation of Tk-RNase H2 by Tk-subtilisin, and then the C-terminal region shifted to the partially or completely resistant forms (I_B-state or I_C-state) to Tk-subtilisin, protecting the N-terminal region. Using pulse proteolysis, the I_B-state became fragment 20 or 22. The I_C-state was tolerant to Tk-subtilisin, showing the intact bands in a tricine−SDS−PAGE gel.

The structural changes in the C-terminus were also observed with an increase in temperature. The native state of Tk-RNase H2 had a large hydrophobic surface at lower temperatures, which decreased with an increase in temperature. However, fragment 20 maintained a small hydrophobic surface at all temperatures (Figure S1A,B of the Supporting Information). Figure 7 shows that fragment 20 maintained native state signal points at each temperature, but only the native state signal points of Tk-RNase H2 were strongly influenced by changes in temperature. Moreover, a steep slope was seen in the baseline prior to the phase transitions of Tk-RNase H2 compared to fragment 20 during the heat-induced unfolding process (Figure 8). These results demonstrated that part of the C-terminal region of Tk-RNase H2 changed with temperature.

In panels A and B of Figure 3, the magnitudes of the bands of fragments 20 and 22 decreased at 30−60 min, but the intact band was unaffected. Furthermore, fragment 9 appeared at these stages as shown in panels A and C of Figure 3. As fragment 9 includes the C-terminal region of Tk-RNase H2, the results indicated that the I_B-state moved to the I_C-state during the unfolding. In the I_C-state, the C-terminal region was more stable than the N-terminal region, so that the state gradually unfolded through the I_D-state, in which the N-terminal region was digested, with fragment 9 accumulating.

As a result, we provide an unfolding and pulse proteolysis pathway for Tk-RNase H2 (Figure 10). In this model, before the reaction with 4 M GdnHCl, the N-state is present and resistant to Tk-subtilisin (Figure 10a). At the early stage of unfolding by 4 M GdnHCl, the N-state of Tk-RNase H2 becomes a form that is completely digested by Tk-subtilisin (I_A-state) (Figure 10b). A proportion of the I_A-state moves to the I_B-state and I_C-state of Tk-RNase H2, which are resistant to Tk-subtilisin during unfolding. Fragments 20 and 22 are observed when the C-terminal region of the I_B-state is digested by Tk-subtilisin. During the middle stages, the N-terminal region of the I_C-state unfolds gradually and is digested in 4 M GdnHCl (Figure 10d).

Origin of Slow Unfolding of Tk-RNase H2. Our results show that the rates of unfolding of fragment 20 were comparable to those of slow unfolding after the burst phase of Tk-RNase H2. This indicated that the unfolding reaction of fragment 20 was rate-limiting in the slow unfolding process of Tk-RNase H2. As fragment 20 is a C-terminal deletion of Tk-RNase H2, the slow unfolding was attributed to the N-terminal region of Tk-RNase H2. In our previous reports on Tk-RNase H2, the hydrophobic residues in the N-terminal region[27] and the buried hydrophobic residues near the surface[29] were found to contribute to slow unfolding. These results suggested that buried hydrophobic residues near the surface in the N-terminal region were possible causes of the slow unfolding of Tk-RNase H2. This hypothesis will be tested in the future by amino acid substitution experiments.

Role of the C-Terminal Region of Tk-RNase H2. The crystal structure of Tk-RNase H2[41] and our experiments show that the C-terminal region has secondary structures under the native condition and at moderate temperatures, whereas the conformation changes occur during the unfolding or with an increase in temperature. In the unfolding, this region shifts to a protease resistant form without native-like secondary structures. The changed conformation is able to protect the N-terminal region against proteolysis. This region does not contribute to the slow unfolding of Tk-RNase H2 but accelerates the folding, suggesting that the C-terminal region folds faster than the N-terminal region.

At higher temperatures, where the host organism, *T. kodakarensis*, can grow, Tk-RNase H2 has a "native conformation". Our results suggest that the native conformation corresponds to the "unfolding intermediate protease resistant form". Muroya et al.[41] showed that the C-terminal region plays an important role in substrate binding and changes the conformation during this process. Therefore, the C-terminal region has no secondary structure but stabilizes the N-terminal region and then moves to make interactions with the substrate at higher temperatures.

■ ASSOCIATED CONTENT

Supporting Information

ANS fluorescence spectra of Tk-RNase H2 and fragment 20 at several temperatures (Figure S1), kinetic unfolding and refolding curves of fragment 20 at 25 °C (Figure S2), thermodynamic stability profiles of Tk-RNase H2 and fragment 20 (Figure S3), and kinetic unfolding curve and pulse proteolysis experiments with Tm-RNase H2 at 25 °C (Figure S4). This material is available free of charge via the Internet at http://pubs.acs.org.

■ AUTHOR INFORMATION

Corresponding Author

*E-mail: takano@kpu.ac.jp. Telephone and fax: +81-75-703-5654.

Funding

This work was supported in part by grants (22710215 and 24380055) from the Ministry of Education, Culture, Sports, Science, and Technology of Japan and by an Industrial Technology Research Grant Program (09A03002) of the New Energy and Industrial Technology Development Organization (NEDO) of Japan.

Notes

The authors declare no competing financial interest.

■ ABBREVIATIONS

Tk-RNase H2, ribonuclease H2 from *T. kodakarensis*; Tk-subtilisin, subtilisin-like serine protease from *T. kodakarensis*; GdnHCl, guanidine hydrochloride; CD, circular dichroism; Pf-PCP, pyrrolidone carboxyl peptidase from *P. furiosus*; Tm-RNase H2, ribonuclease H2 from *Th. maritima*; TCA, trichloroacetic acid; ANS, anilino-8-naphthalenesulfonic acid; SDS−PAGE, sodium dodecyl sulfate−polyacrylamide gel electrophoresis.

■ REFERENCES

(1) Kim, P. S., and Baldwin, R. L. (1990) Intermediates in the folding reactions of small proteins. *Annu. Rev. Biochem. 59*, 631−660.

(2) Kuwajima, K., Nitta, K., Yoneyama, M., and Sugai, S. (1976) Three-state denaturation of α-lactalbumin by guanidine hydrochloride. *J. Mol. Biol. 106*, 359−373.

(3) Ptitsyn, O. B. (1995) Molten globule and protein folding. *Adv. Protein Chem. 47*, 83−229.

(4) Baldwin, R. L., Frieden, C., and Rose, G. D. (2010) Dry molten globule intermediates and the mechanism of protein unfolding. *Proteins: Struct., Funct., Genet. 78*, 2725−2737.

(5) Arai, M., and Kuwajima, K. (1996) Rapid formation of a molten globule intermediate in refolding of lactalbumin. *Folding Des. 1*, 275−287.

(6) Udgaonkar, J. B., and Baldwin, R. L. (1988) NMR evidence for an early framework intermediate on the folding pathway of ribonuclease A. *Nature 335*, 694−699.

(7) Roder, H., Elove, G. A., and Englander, S. W. (1988) Structural characterization of folding intermediates in cytochrome c by H-exchange labelling and proton NMR. *Nature 335*, 700−704.

(8) Balbach, J., Forge, V., van, Nuland, N. A., Winder, S. L., Hore, P. J., and Dobson, C. M. (1995) Following protein folding in real time using NMR spectroscopy. *Nat. Struct. Biol. 2*, 865−870.

(9) Eliezer, D., Jennings, P. A., Wright, P. E., Doniach, S., Hodgson, K. O., and Tsuruta, H. (1995) The radius of gyration of an apomyoglobin folding intermediate. *Science 270*, 487−488.

(10) Arai, M., Ikura, T., Semisotnov, G. V., Kihara, H., Amemiya, Y., and Kuwajima, K. (1998) Kinetic refolding of β-lactoglobulin. Studies by synchrotron X-ray scattering, and circular dichroism, absorption and fluorescence spectroscopy. *J. Mol. Biol. 275*, 149−162.

(11) Serrano, L., Matouschek, A., and Fersht, A. R. (1992) The folding of an enzyme. III. Structure of the transition state for unfolding of barnase analysed by a protein engineering procedure. *J. Mol. Biol. 224*, 805−818.

(12) Cavagnero, S., Debe, D. A., Zhou, Z. H., Adams, M. W. W., and Chan, S. I. (1998) Kinetic role of electrostatic interactions in the unfolding of hyperthermophilic and mesophilic rubredoxins. *Biochemistry 37*, 3369−3376.

(13) Ogasahara, K., Nakamura, M., Nakura, S., Tsunasawa, S., Kato, I., Yoshimoto, T., and Yutani, K. (1998) The unusually slow unfolding rate causes the high stability of pyroolidone carboxyl peptidase from a hyperthermophilile *Pyrococcus furiosus*: Equilibrium and kinetic studies of guanidine hydrochloride-induced unfolding and refolding. *Biochemistry 37*, 17537−17544.

(14) Dams, T., and Jaenicke, R. (1999) Stability and folding of dihydrofolate reductase from the hyperthermophilic bacterium *Thermotoga maritime*. *Biochemistry 38*, 9169−9178.

(15) Kaushik, J. K., Ogasahara, K., and Yutani, K. (2002) The unusually slow relaxation kinetics of the folding-unfolding of pyrrolidone carboxyl peptidase from a hyperthermophile *Pyrococcus furiosus*. *J. Mol. Biol. 316*, 991−1003.

(16) Jaswal, S. S., Sohl, J. L., Dans, J. H., and Agard, D. A. (2002) Energetic landscape of α-lytic protease optimizes longevity through kinetic stability. *Nature 415*, 343−346.

(17) Zeeb, M., Lipps, G., Lilie, H., and Balbach, J. (2004) Folding and association of an extremely stable dimeric protein from *Sulfolobus islandicus*. *J. Mol. Biol. 336*, 227−240.

(18) Forrer, P., Chang, C., Ott, D., Wlodawer, A., and Pluckthun, A. (2004) Kinetic stability and crystal structure of the viral capside protein SHP. *J. Mol. Biol. 344*, 179−193.

(19) Wittung-Stafshede, P. (2004) Slow unfolding explains high stability of thermostable ferredoxins: Common mechanism governing thermostability? *Biochim. Biophys. Acta 1700*, 1−4.

(20) Duy, C., and Fitter, J. (2005) Thermostability of irreversible unfolding α-amylases analyzed by unfolding kinetics. *J. Biol. Chem. 280*, 37360−37365.

(21) Kaushik, J. K., Iimura, S., Ogasahara, K., Yamagata, Y., Segawa, S., and Yutani, K. (2006) Completely buried, non-ion-paired glutamic acid contributes favorably to the conformational stability of pyrrolidone carboxyl peptidases from hyperthermophiles. *Biochemistry 45*, 7100−7112.

(22) Mishra, R., Olofsson, L., Karlsson, M., Carlsson, U., Nicholls, I. A., and Hammarstrom, P. (2008) A conformationally isoformic thermophilic protein with high kinetic unfolding barriers. *Cell. Mol. Life Sci. 65*, 827−839.

(23) Costas, M., Rodriguez-Larrea, D., De Maria, L., Borchert, T. V., Gomez-Puyou, A., and Sanchez-Ruiz, J. M. (2009) Between-species variation in the kinetic stability of TIM proteins linked to solvation-barrier free energies. *J. Mol. Biol. 385*, 924−937.

(24) Iimura, S., Yagi, H., Ogasahara, K., Akutsu, H., Noda, Y., Segawa, S., and Yutani, K. (2004) Unusually slow denaturation and refolding process of pyrrolidone carcoxyl peptidase from a hyper-thermophile are highly cooperative: Real-time NMR studies. *Biochemistry 43*, 11906−11915.

(25) Mukaiyama, A., Takano, K., Haruki, M., Morikawa, M., and Kanaya, S. (2004) Kinetically robust monomeric protein from a hyperthermophile. *Biochemistry 43*, 13859−13866.

(26) Mukaiyama, A., and Takano, K. (2009) Slow unfolding of monomeric proteins from hyperthermophiles with reversible unfolding. *Int. J. Mol. Sci. 10*, 1369−1385.

(27) Dong, H., Mukaiyama, A., Tadokoro, T., Koga, Y., Takano, K., and Kanaya, S. (2008) Hydrophobic effect on the stability and folding of a hyperthermophilic protein. *J. Mol. Biol. 378*, 264−272.

(28) Takano, K., Higashi, R., Okada, J., Mukaiyama, A., Tadokoro, T., Koga, Y., and Kanaya, S. (2008) Proline effect on the thermostability and slow unfolding of a hyperthermophilic protein. *J. Biochem. 145*, 79−85.

(29) Okada, J., Okamoto, T., Mukaiyama, A., Tadokoro, T., You, D. J., Koga, Y., Takano, K., and Kanaya, S. (2010) Evolution and thermodynamics of slow unfolding of hyperstable monomeric proteins. *BMC Evol. Biol. 10*, 207.

(30) Tanaka, S., Saito, K., Chon, H., Matsumura, H., Koga, Y., Takano, K., and Kanaya, S. (2007) Crystal structure of unautoprocessed precursor of subtilisin from a hyperthermophilic archaeon: Evidence for Ca^{2+}-induced folding. *J. Biol. Chem. 282*, 8246−8255.

(31) Laemmli, U. K. (1970) Cleavage of Structural Proteins during the Assembly of the Head of Bacteriophage T4. *Nature 227*, 680−685.

(32) Goodwin, T. W., and Morton, R. A. (1946) The spectrophotometric determination of tyrosine and tryptophan in proteins. *Biochem. J. 40*, 628−632.

(33) Schägger, H. (2006) Tricine-SDS-PAGE. *Nat. Protoc. 1*, 16−22.

(34) Santoro, M. M., and Bolen, B. W. (1988) Unfolding free energy changes determined by the linear extrapolation method. 1. Unfolding of phenylmethanesulfonyl α-chymotrypsin using different denaturants. *Biochemistry 27*, 8063−8068.

(35) Park, C., and Marqusee, S. (2005) Pulse proteolysis: A simple method for quantitative determination of protein stability and ligand binding. *Nat. Methods 2*, 207−212.

(36) Na, Y. R., and Park, C. (2009) Investigating protein unfolding kinetics by pulse proteolysis. *Protein Sci. 18*, 268−276.

(37) Chang, Y., and Park, C. (2009) Mapping transient partial unfolding by protein engineering and native-state proteolysis. *J. Mol. Biol. 393*, 543−556.

(38) Kim, M. S., Song, J., and Park, C. (2009) Determining protein stability in cell lysates by pulse proteolysis and Western blotting. *Protein Sci. 18*, 1051−1059.

(39) Semisotnov, G. V., Rodionova, N. A., Kutyshenko, V. P., Ebert, B., Blanck, J., and Ptitsyn, O. B. (1987) Sequential mechanism of refolding of carbonic anhydrase B. *FEBS Lett. 224*, 9−13.
(40) Kuwajima, K. (1989) The molten globule state as a clue for understanding the folding and cooperativity of globular-protein structure. *Proteins: Struct., Funct., Genet. 6*, 87−103.
(41) Muroya, A., Tsuchiya, D., Ishikawa, M., Haruki, M., Morikawa, M., Kanaya, S., and Morikawa, K. (2001) Catalytic center of an archaeal type 2 ribonuclease H as revealed by X-ray crystallographic and mutational analyses. *Protein Sci. 10*, 707−714.